ECS Journal of Solid State Science and Technology, **2** (8) N3041-N3044 (2013)
2162-8769/2013/2(8)/N3041/4/$31.00 © The Electrochemical Society

JSS Focus Issue on Wide Bandgap Power Semiconductors

Hydrogen Incorporation Dependence on the Thermal Growth Route in Dielectric/SiC Structures

Silma A. Corrêa,[a,z] Gabriel V. Soares,[a,b,*] Philip Tanner,[c] Jisheng Han,[c] Sima Dimitrijev,[c] and Fernanda C. Stedile[a,d]

[a]*PGMICRO, Universidade Federal do Rio Grande do Sul, Porto Alegre, RS 91509-900, Brazil*
[b]*Instituto de Física, Universidade Federal do Rio Grande do Sul, Porto Alegre, RS 91509-900, Brazil*
[c]*Queensland Micro- and Nanotechnology Centre and Griffith School of Engineering, Griffith University, Nathan, Queensland 4111, Australia*
[d]*Instituto de Química, Universidade Federal do Rio Grande do Sul, Porto Alegre, RS 91509-900, Brazil*

The incorporation of hydrogen in dielectric/SiC structures and Pt/dielectric/SiC structures whose dielectric films were thermally grown in O_2, NO, or O_2 followed by annealing in NO was investigated. The amount and the distribution of hydrogen incorporated and the capacitance-voltage characteristics were observed to be dependent on the thermal growth route employed. Hydrogen was mainly incorporated in the dielectric film/SiC interface region and larger amounts were incorporated when the Pt electrode was used. Annealing in hydrogen increased the negative shift in the flatband voltage, which was more pronounced when the Pt electrode was used in the case of NO-annealed SiO_2/SiC sample.
 [DOI: 10.1149/2.009308jss]

Manuscript submitted March 7, 2013; revised manuscript received June 14, 2013. Published June 26, 2013. *This paper is part of the JSS Focus Issue on Wide Bandgap Power Semiconductors.*

To overcome the limits of silicon-based power devices, new semiconductor materials are necessary. Silicon carbide (SiC) is a wide bandgap semiconductor that presents adequate properties for high-power, high-temperature, and high-frequency electronics. These characteristics have been recently explored in the first commercially available metal-oxide-semiconductor field effect transistors (MOSFETs).[1] However, reducing the density of electron traps at and near the SiO_2/semiconductor interface, to improve the channel carrier mobility[2] and reliability of MOSFET devices, still remains as the main technological challenge.[3,4]

The high density of interface states (D_{it}) in the SiO_2/SiC interface region has been attributed to carbon related defects generated during the thermal oxidation of the SiC.[5–7] In order to improve the quality of this interface, post-oxidation annealing (POA) in nitric oxide (NO) has been employed as a successful method to reduce D_{it} and to improve device reliability.[4,8] The effect of the incorporation of N was related to both the removal and the passivation of residual C in the dielectric/SiC interface region.[9–11] The use of POA in H_2 also led to reduction in D_{it} below the conduction band for n-type 4H-SiC (0001) MOS structures[12] and improve the channel mobility of 4H-SiC (0001) MOSFETs.[13] Moreover, combining POAs in NO and in H_2 using platinum (Pt) as the electrode metal caused a complementary reduction in D_{it} [10,14] and enhanced field-effect mobility in 4H-SiC (0001) MOSFETs[15] compared with only NO or only H_2 annealings.

The passivation effect of POA in H_2 has been investigated only in the case of thermal growth in O_2 with and without POA in NO, but the consequences of POA in H_2 in dielectric films directly grown in NO still remain unknown. Results for dielectric films grown on the carbon face of the SiC single-crystal indicate that the direct growth in NO led to better breakdown characteristics than NO-annealed oxides.[3] Reliability results for silicon-faced 4H-SiC by Jamet et al.[9] also revealed that dielectric films grown directly in NO exhibit a higher resistance to high field stress than previously grown dry oxide films annealed in NO. Furthermore, MOS structures with dielectric films grown in NO presented superior capacitance-voltage (C-V) characteristics than SiO_2/SiC annealed in NO.[16,17] Therefore, the understanding of the consequences of combining the thermal growth in NO and POA in H_2, along with a systematic investigation of the influence of the dielectric film growth process and the use of a Pt electrode, on the incorporation of hydrogen in dielectric/SiC structures are important issues in order to achieve further improvements in the electrical properties of SiC-based devices. In this work we report results of physicochemical and C-V characterization of dielectric/SiC structures grown by different thermal processes and annealed in H_2 with or without a Pt electrode. The correlation between atomic composition, hydrogen distribution, and electrical characteristics is also presented.

Experimental

Silicon-faced (0001) n-type 4° off-axis 4H-SiC wafers with nitrogen-doped 4.5 μm thick epitaxial layers to a concentration of 1.4×10^{16} at.cm^{-3} purchased from Cree were cleaned in a mixture of H_2SO_4 and H_2O_2 followed by the RCA process. After etch in a 5% HF aqueous solution for 1 min, samples were loaded in a quartz tube furnace. Three different routes were used to grow dielectric films on SiC. SiO_2 films were grown at 1100°C for 4 h in a 100 mbar static atmosphere of O_2 isotopically enriched to 97% in the ^{18}O isotope (O_2-route). Silicon oxynitride film growth in NO (NO-route) or NO-annealing of $Si^{18}O_2$/SiC (O_2/NO-route) were performed at 1250°C for 2 h at a NO flow rate of 0.1 SLM. Concerning H_2 annealing temperature, previous works reported improvement in D_{it} and channel mobility for 4H-SiC (0001) MOSFETs using POA in hydrogen at temperatures $\geq$ 800°C.[12,13,18] On the other hand, the quality of the Pt electrode degrades at anneal temperatures greater than 600°C.[19] Therefore, in the present work, annealings in H_2 were performed at 600°C for 1 h in a 200 mbar static atmosphere enriched to 99.8% in the ^2H (^2H = D) isotope, termed D_2 anneal. After the annealing and the system has reached room temperature, the D_2 atmosphere was removed by pumping the system down to $\sim 10^{-5}$ mbar. The use of hydrogen atmosphere enriched in the deuterium isotope (^2H = D) assumes that it mimics the behavior of the ^1H. Platinum (Pt) was chosen as the metal electrode due to its catalytic effect in dissociating H_2 molecules into atomic hydrogen,[10] which is more likely to be incorporated than molecular hydrogen.

To evaluate the influence of the presence of Pt in the incorporation of hydrogen, in some samples Pt electrodes were deposited via DC sputtering before the D_2 anneal. Samples analyzed by Nuclear Reaction Analyzes (NRA) had their entire surfaces covered by Pt while on samples used in C-V measurements circular Pt electrodes (0.0025 cm^2) were deposited. Some samples had the Pt electrode removed using a HCl + HNO_3 (3:1) solution and/or the dielectric film removed by HF solution after the D_2 anneal and before being analyzed by NRA to detect D. The use of ^{18}O and D rare isotopes (natural abundances of 0.2 and 0.015%, respectively) allows one to

*Electrochemical Society Active Member.
zE-mail: silma.alberton@ufrgs.br

distinguish them from O and H incorporated during air exposure and/or NO annealing. ^{18}O and D quantifications were accomplished by nuclear reaction analyzes using the $^{18}O(p,\alpha)^{15}N$ nuclear reaction[20] at 730 keV (10^{13} $^{18}O.cm^{-2}$ sensitivity and 5% accuracy) and the $D(^3He,p)^4He$ nuclear reaction[21] at 700 keV (10^{12} $D.cm^{-2}$ sensitivity and 10% accuracy). The areal density of ^{16}O was determined by Rutherford backscattering spectrometry in channeling geometry (c-RBS) using He^+ ions of 1 MeV,[22] with 10^{14} $^{16}O.cm^{-2}$ sensitivity and 10% accuracy. Oxygen areal densities were converted into SiO_2 film thicknesses using the relationship: 10^{15} $O.cm^{-2} = 0.226$ nm of SiO_2, valid for 2.21 $g.cm^{-3}$ dense SiO_2 films.[20]

MOS capacitors with platinum electrodes were fabricated to enable C-V measurements (10 kHz frequency) that were performed at room temperature, with the electrode bias swept from accumulation to depletion. Aluminum was also sputtered on the back of the sample to make a large area contact using a Surrey NanoSystems γ-1000C. HFCV characteristics were obtained at the sweep rate of 0.1 V/s using a computer controlled HP4284A LCR meter. Theoretical low frequency and deep depletion C-V data were calculated based on the standard equations for metal-oxide-semiconductor structures.[23] Using the standard electronic properties of 4H-SiC, the oxide thickness and SiC doping concentration were the parameters adjusted to fit the theoretical data to the experimental curve.

Results and Discussion

Dielectric films grown according to each growth route were characterized using ion beam analysis techniques. Results of ^{18}O and ^{16}O quantification are shown in Table I along with the estimated film thickness as detailed above. One can notice that when the $^{18}O_2$ atmosphere was employed, ^{16}O was not observed, within the detection limit of the RBS technique. However, in the case of thermal growth in natural NO, a tiny amount of ^{18}O was observed due to the higher detection limit of the NRA technique. This amount of ^{18}O corresponds to the natural abundance of this nuclide in an 18 nm thick SiO_2 film. When thermal growth was performed in $^{18}O_2$ followed by annealing in NO (O_2/NO-route), areal densities of ^{18}O and ^{16}O reveal total isotopic exchange between the ^{16}O from the NO gas and the ^{18}O from $Si^{18}O_2$ film grown in $^{18}O_2$. In this case, the ^{18}O amount observed can again be attributed to its natural abundance. These results indicate that oxygen atoms in the oxide are highly mobile during NO annealing and that the effect of this treatment is not limited to the dielectric film/SiC interface region, since compositional modification of the whole dielectric film is occurring.

The influence of the thickness of the Pt electrode in the incorporation of D was evaluated. The amount of D that was incorporated in SiO_2/SiC samples with the surface covered by Pt electrode films 10, 20, and 100 nm thick was $(1.2 \pm 0.1) \times 10^{13}$ $D.cm^{-2}$. Since the amount of incorporated D did not depend on the Pt electrode film thickness, i.e., it did not increase as the thickness of the electrode increased, one can conclude that it was not incorporated in the whole depth of the Pt film. In a previous work from our group[24] it was determined that the D incorporated in the Pt electrode film in Pt/SiO_2/SiC structures was located in the Pt/dielectric film interface region. Therefore, we suggest that the D observed in the Pt electrode film was incorporated in this Pt/dielectric film interface region.

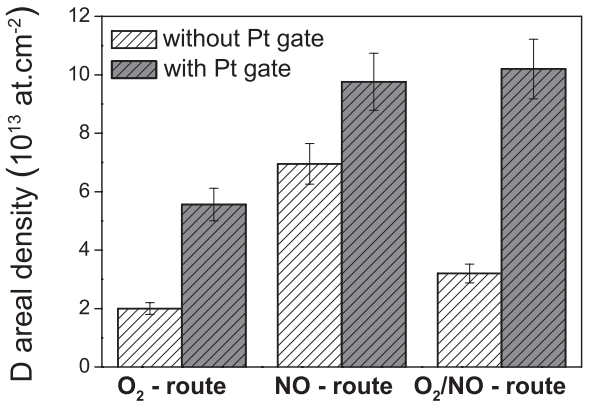

Figure 1. Deuterium areal densities incorporated in dielectric/SiC structures with and without the presence of the Pt electrode for each thermal growth route employed. Error bars correspond to experimental accuracy of 10%.

The influence of the thermal route employed in the growth of dielectric films and the presence of the Pt electrode in the incorporation of hydrogen were also investigated. The total amounts of D incorporated by each growth route with and without a 10 nm thick Pt electrode, as determined by NRA, are shown in Fig. 1. One can notice that, in all cases, larger amounts of D were incorporated in the Pt/dielectric/SiC structures compared with their counterparts without the presence of the Pt electrode. These larger amounts cannot be attributed only to D incorporation in the Pt electrode film, since it was $(1.2 \pm 0.1) \times 10^{13}$ $D.cm^{-2}$ for the three growth routes, which was evaluated by comparison of areal densities observed in samples with the presence of Pt (results shown in Fig. 1) and after the electrode has been removed (3rd column in Table II). It is remarkable that D incorporation is highly dependent on the route employed in the thermal growth of the dielectric films. The sample with the dielectric film thermally grown according to the O_2-route was the one that presented the lowest amount of D incorporated, with and without the presence of Pt. In the case of thermal growth in O_2 followed by NO anneal (O_2/NO-route) a larger amount of D was incorporated than in the case of non-annealed sample, which indicates that the presence of N introduces new sites for D incorporation. Wang et al.[14] combined experimental data and first-principles calculations to propose that nitridation of the SiO_2/SiC interface followed by its hydrogenation leads to the formation of a $SiO_xN_yC_z(H)$ interlayer. The largest amount of D,

Table I. ^{18}O and ^{16}O total amounts and film thicknesses determined by NRA and c-RBS for dielectric films thermally grown according to distinct specified routes. Film thicknesses were determined assuming that the density of the SiO_2 film on SiC is 2.21 $g.cm^{-3}$.

Sample	^{18}O (10^{15} at.cm^{-2})	^{16}O (10^{15} at.cm^{-2})	Thickness (nm)
$^{18}O_2$ – route	42.79 ± 2.25	*	9.5
NO – route	0.16 ± 0.01	73.1 ± 7.3	16.5
$^{18}O_2$/NO – route	0.18 ± 0.01	96.2 ± 9.6	21.7

*Below the sensitivity limit of the c-RBS technique.

Table II. Deuterium areal densities in the dielectric films were determined by NRA for each growth route. The presence of a Pt electrode during D_2 anneal is indicated (2nd column), but this Pt layer was removed before D quantification when it was present. D total amounts incorporated in the whole depth of the dielectric films (3rd column), after the dielectric films thicknesses have been reduced to ∼4 nm (4th column), and after the removal of the dielectric films by long etchings in HF solution (5th column).

Sample	Pt electrode	D (10^{13} at.cm^{-2}) As grown dielectric film	D (10^{13} at.cm^{-2}) ∼4 nm dielectric film	D (10^{13} at.cm^{-2}) Removed dielectric film
$^{18}O_2$ – route	Yes	4.4 ± 0.4	3.7 ± 0.4	*
	No	2.0 ± 0.2	2.1 ± 0.2	*
NO – route	Yes	8.6 ± 0.9	7.5 ± 0.7	5.3 ± 0.5
	No	7.0 ± 0.7	6.0 ± 0.6	3.4 ± 0.3
$^{18}O_2$/NO – route	Yes	8.9 ± 0.9	5.2 ± 0.5	2.0 ± 0.2
	No	3.2 ± 0.3	2.0 ± 0.2	*

*Below the sensitivity limit of the NRA technique.

comparing samples without the Pt electrode, was observed in the sample with the dielectric film directly grown in NO (NO-route), which is another indication that D is being incorporated in N-related sites. Chakraborty et al.[17] reported the presence of larger amounts of N in the case of dielectric films grown directly in NO compared with dry SiO_2 film annealed in NO, which could explain the largest amount of D that was incorporated in the sample with the dielectric film grown according to the NO-route. Regarding samples with D_2 anneal after the deposition of the Pt electrode, no pronounced difference between the amounts of D incorporated in samples with dielectric films grown according to NO- and to O_2/NO-routes was observed.

In order to evaluate the distribution of D within the dielectric film and in the dielectric film/SiC interface region, areal densities of D were determined after reducing the dielectric film thickness to ∼4 nm and also after removal of the dielectric film by a long etching in HF solution. The total amounts of D incorporated by each growth route and in different dielectric film thickness, as determined by NRA, are shown in Table II. In samples that were submitted to D_2 annealing in the presence of the Pt electrode, D amounts were determined after the Pt layer has been removed. One can notice that in these samples larger amounts of D were incorporated in the dielectric film compared with their counterparts annealed without the presence of a Pt electrode. For all samples, D was mainly incorporated in the dielectric film/SiC interface region. In the case of thermal growth in O_2 without the presence of a Pt electrode, D was only incorporated in the dielectric film/SiC interface region, since the same amounts of D were observed for the non-etched dielectric film and for the 4 nm thick film. A previous work by Soares et al.[25] also reported that for SiO_2/SiC structures submitted to D_2 anneal at 600°C, without a Pt electrode, all D was incorporated in the SiO_2/SiC interface region. The D incorporation in dielectric films grown according to the NO-route reveals that even after a reduction of ∼4 times in the film thickness (the original thickness was 16.5, as shown in Table I), only a ∼15% reduction in the amount of D was observed, in samples with and without the Pt electrode. In the case of thermal growth in O_2 followed by NO anneal, for samples with and without the Pt electrode, the amount of D incorporated in the dielectric film/SiC interface region (∼4 nm thick dielectric film) represents 60% of the amount incorporated in whole film, although this thickness represents less than 20% of the total film (see Table I). It is noteworthy that after the removal of the dielectric films by etching, no D was observed within the detection limit of the nuclear reaction analysis in samples with the dielectric film thermally grown according to the O_2-route. In the case of thermal growth in O_2 followed by NO anneal (O_2/NO-route), D was observed after the removal of the dielectric film only in the case of D_2 anneal in the presence of a Pt electrode. This amount stands for 22% of the amount that was incorporated considering the whole dielectric film. In samples with the dielectric film thermally grown directly in NO (NO-route), ∼60% and ∼50% of the D incorporated, for samples with and without the Pt electrode, respectively, remain even after the removal of the dielectric film. The distinct remaining amounts of D that were observed for each growth route indicate that they led to the formation of interfaces with different compositions and affinities with hydrogen. In a previous work,[11] we presented results from X-ray photoelectron spectroscopy (XPS) and X-ray reflectometry (XRR) evidencing that the interfacial layer of silicon oxycarbide compounds (SiO_xC_y) formed during the thermal growth of dielectric films on SiC was modified by the incorporation of N due to NO annealings. The thickness of this interfacial layer was drastically reduced in the case of thermal growth directly in NO. An intermediate thickness was observed when the dielectric film was grown in O_2 followed by NO anneal, as compared to a film grown only in O_2. Recently, Kosugi et al.[4] reported XPS results from NO annealed (0001) 4H-SiC surfaces revealing the incorporation of N atoms with an areal density of 10^{14} cm^{-2} that remain fixed in the interface region even after the removal of the oxide layer by etching in HF. It is noteworthy that silicon oxycarbide compounds present high chemical inertness, not being removed by HF solution as well as by several other acid and oxidizing wet etchings.[26] Therefore, fixed N observed after HF etching might be related with its incorporation in the silicon oxycarbide interfacial layer. The presence of larger amounts of D in the dielectric film/SiC interface region that remain after the removal of the dielectric film by etching, observed for samples grown by the NO-route compared with the other thermal growth routes investigated, could be a consequence of its incorporation in these N-related sites in the interfacial layer that contains Si, C, O, and N.

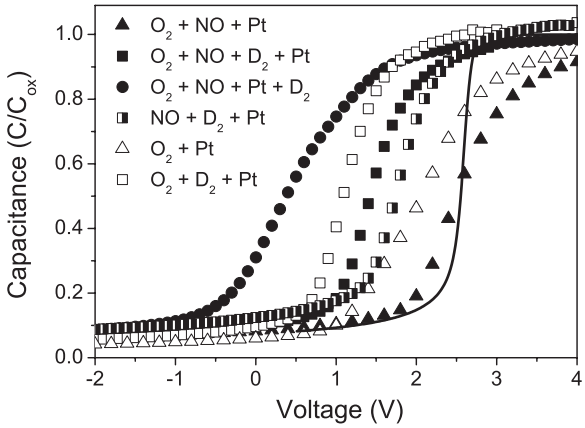

Figure 2. C-V curves for Pt/dielectric film/4H-SiC (0001) MOS capacitors with dielectric films grown according to O_2-, NO-, and O_2/NO-routes. The sequence of treatments and corresponding symbols are indicated in the inset. Ideal C-V curve (solid black line) is also presented for comparison. The ideal flatband voltage is +2.56 V.

C-V curves for MOS capacitors with dielectric films grown according to different thermal growth routes are shown in Fig. 2. The ideal C-V curve was calculated assuming the vacuum value for the work-function of the Pt electrode. Nevertheless, the possibility of reduction in the effective work-function of the Pt due to the formation of a D-induced dipole layer in the Pt/dielectric interface, as reported by Lundström and DiStefano,[27] cannot be ruled out in the case of samples that underwent a D_2 anneal in the presence of the Pt electrode. The curve for the sample that was oxidized but not submitted to an annealing in D_2 (open triangles) presents a negative shift (−0.63 V) in the flatband-voltage (V_{FB}) as compared to the ideal curve due to the presence of positive effective charge. After annealing in D_2, an even larger negative shift (−1.52 V) in the V_{FB} was observed (open squares). These results evidence that annealings in D_2 led to an increase in the positive effective charge. A similar behavior was also reported by Stein von Kamienski et al.[28]: they observed the formation of positive oxide charge after forming gas anneals of dry oxide samples. The sample thermally grown in O_2 followed by NO anneal (full triangles) does not exhibit a V_{FB} shift. Therefore, the annealing in NO reduced the positive effective charge compared with the thermal growth only in O_2. However, negative V_{FB} shifts were observed in the case of dielectric films thermally grown in O_2 followed by NO submitted to annealing in D_2 with (full circles) and without (full squares) the presence of Pt electrode, being −2.13 V and −1.12 V, respectively. Concerning the NO sample annealed in D_2 without the presence of a Pt electrode (half filled squares), a V_{FB} shift of −0.69 V was observed, being smaller than the observed for the other thermal growth routes (full and open squares). C-V curves of the O_2 and the NO samples annealed in D_2 in the presence of Pt (O_2 + Pt + D_2 and NO + Pt + D_2) are not shown because they did not reach a saturation level in the accumulation region, indicating that the dielectric films became leaky after D_2 anneal in the presence of Pt. The sample with the dielectric film grown in O_2 followed by annealing in NO that was submitted to D_2 anneal in the presence of Pt (O_2 + NO + Pt + D_2) reached saturation level in the accumulation, as shown in Fig. 2 (full circles), indicating that this film, which is thicker than those grown by O_2- and NO-routes, is less susceptible to present leakage problems. Nevertheless, the possibility of leakage in the dielectric films being

caused by damage in the dielectric film/Pt interface due to D_2 anneal cannot be ruled out.

Therefore, results indicate that instead of being beneficial, the incorporation of D in the presence of the Pt film was deleterious in the case of thermal growth routes investigated. In the light of these results, no D_{it} or channel mobility measurements were performed on samples. However, some inferences can be made from the slope of the C-V curves. In the case of O_2/NO samples, after annealing in D_2 in the presence of Pt (full circles), the D_{it} was increased as indicated by the reduced slope of the C-V curve near the depletion region. On the other hand, based on the slope of the C-V curves for O_2 (open triangles and squares) and O_2/NO samples (solid triangles and squares), a reduction in D_{it} after annealing in D_2 without the presence of a Pt electrode can be inferred.

Conclusions

The influence of the thermal growth process and the presence of a platinum electrode on the incorporation and distribution of hydrogen in SiO_xN_y/SiC and Pt/SiO_xN_y/SiC structures were investigated. Results evidenced that NO annealing led to total isotopic exchange between ^{16}O from the gas phase ($N^{16}O$) and ^{18}O from the previous $Si^{18}O_2$ film, evidencing the large mobility of this element in the system. Samples with dielectric films thermally grown in O_2 presented the lowest amounts of D incorporated with and without a Pt electrode. In samples that underwent NO treatments, the presence of a Pt electrode led to similar amounts of D incorporated, whereas without Pt, the sample directly grown in NO exhibits the largest amount of D incorporated. In all samples, D was mainly incorporated in the dielectric film/SiC interface region. Besides, D was observed even after the removal of the dielectric films in the case of thermal growth directly in NO and for the O_2/NO sample with the D_2 anneal performed in the presence of a Pt electrode. Flatband voltage was observed to be dependent on the thermal growth route employed. Annealing in D_2 increased the negative shift in the flatband voltage, which was more pronounced when the Pt electrode was used, in the case of NO anneal following the thermal growth in O_2.

Acknowledgments

The authors thank MCT/CNPq, INCTs NAMITEC and INES, CAPES, and FAPERGS for financial support.

References

1. L. Cheng, S.-H. Ryu, A. K. Agarwal, M. O'Loughlin, A. Burk, J. Richmond, A. Lelis, C. Scozzie, and J. W. Palmour, *Mater. Sci. Forum*, **717–720**, 1065 (2012).
2. T. E. Rudenko, I. N. Osiyuk, I. P. Tyagulski, H. Ö. Ólafsson, and E. Ö. Sveinbjörnsson, *Solid-State Electron.*, **49**, 545 (2005).
3. Z. Chen, A. C. Ahyi, X. Zhu, M. Li, T. Isaacs-Smith, J. R. Williams, and L. C. Feldman, *J. Electron. Mater.*, **39**, 526 (2010).
4. R. Kosugi, T. Umeda, and Y. Sakuma, *Appl. Phys. Lett.*, **99**, 182111 (2011).
5. V. V. Afanas'ev, M. Bassler, G. Pensl, and M. Schulz, *Phys. Status Solidi A*, **162**, 321 (1997).
6. J. L. Cantin, H. J. V. Bardeleben, Y. Shishkin, Y. Ke, R. P. Devaty, and W. J. Choyke, *Phys. Rev. Lett.*, **92**, 015502 (2004).
7. K. C. Chang, N. T. Nuhfer, L. M. Porter, and Q. Wahab, *Appl. Phys. Lett.*, **77**, 2186 (2000).
8. H. Li, S. Dimitrijev, H. B. Harrison, and D. Sweatman, *Appl. Phys. Lett.*, **70**, 2028 (1997).
9. P. Jamet, S. Dimitrijev, and P. Tanner, *J. Appl. Phys.*, **90**, 5058 (2001).
10. S. Dhar, L. C. Feldman, S. Wang, T. Isaacs-Smith, and J. R. Williams, *J. Appl. Phys.*, **98**, 14902 (2005).
11. S. A. Corrêa, C. Radtke, G. V. Soares, L. Miotti, I. J. R. Baumvol, S. Dimitrijev, J. Han, L. Hold, F. Kong, and F. C. Stedile, *Appl. Phys. Lett.*, **94**, 251909 (2009).
12. K. Fukuda, S. Suzuki, T. Tanaka, and K. Arai, *Appl. Phys. Lett.*, **76**, 1585 (2000).
13. S. Suzuki, W. J. Cho, R. Kosugi, J. Senzaki, S. Harada, and K Fukuda, *Mater. Sci. Forum*, **353–356**, 643 (2001).
14. S. Wang, S. Dhar, S. R. Wang, A. C. Ahyi, A. Franceschetti, J. R. Williams, L. C. Feldman, and S. T. Pantelides, *Phys. Rev. Lett.*, **98**, 26101 (2007).
15. S. Dhar, S. Wang, J. R. Williams, S. T. Pantelides, and L. C. Feldman, *Mater. Res. Bull.*, **30**, 288 (2005).
16. G. V. Soares, I. J. R. Baumvol, L. Hold, F. Kong, J. Han, S. Dimitrijev, C. Radtke, and F. C. Stedile, *Appl. Phys. Lett.*, **91**, 041906 (2007).
17. S. Chakraborty, P. T. Lai, and P. C. K. Kwok, *Microelectron. Reliab.*, **42**, 455 (2002).
18. W. J. Cho, R. Kosugi, K. Fukuda, K. Arai, and S. Suzuki, *Appl. Phys. Lett.*, **77**, 1215 (2000).
19. S. Dhar, PhD dissertation, Vanderbilt University (2004).
20. I. J. R. Baumvol, *Surf. Sci. Rep.*, **36**, 1 (1999).
21. I. J. R. Baumvol, E. P. Gusev, F. C. Stedile, F. L. Freire Jr., M. L. Green, and D. Brasen, *Appl. Phys. Lett.*, **72**, 450 (1998).
22. L. C. Feldman, J. W. Mayer, and S. T. Picraux, *Materials Analysis by Ion Channeling* (Academic Press, New York, 1982).
23. D. K. Schroder, *Semiconductor Material and Device Characterization* (Wiley Interscience, New York, 1998), p. 339.
24. F. C. Stedile, G. V. Soares, I. J. R. Baumvol, C. Radtke, R. Loloee, and R. N. Ghosh, In. *Proceedings of the International Conference on Silicon Carbide and Related Materials*, Otsu, Japan, 2007.
25. G. V. Soares, I. J. R. Baumvol, C. Radtke, and F. C. Stedile, *Appl. Phys. Lett.*, **90**, 081906 (2007).
26. S. A. Corrêa, C. Radtke, G. V. Soares, I. J. R. Baumvol, C. Krug, and F. C. Stedile, *Electrochem. Solid-State Lett.*, **11**, H258 (2008).
27. I. Lundström and T. DiStefano, *Solid State Commun.*, **19**, 871 (1976).
28. E. Stein von Kamienski, A. Gölz, and H. Kurz, *Mater. Sci. Eng. B*, **29**, 131 (1995).